

## Article

# High Spatial and Temporal Resolution Methane Emissions Inventory from Terrestrial Ecosystems in China, 2010–2020

Yongliang Yang<sup>1,2</sup> and Yusheng Shi<sup>1,\*</sup> 

<sup>1</sup> State Environmental Protection Key Laboratory of Satellite Remote Sensing, Aerospace Information Research Institute, Chinese Academy of Sciences, Beijing 100101, China

<sup>2</sup> College of Resources and Environment, University of Chinese Academy of Sciences, Beijing 101408, China

\* Correspondence: shiys@aircas.ac.cn; Tel.: +86-10-6485-2835

**Abstract:** Methane (CH<sub>4</sub>) is not only an important greenhouse gas next to carbon dioxide (CO<sub>2</sub>), but also an important chemically active gas. Under the background of climate warming, the measurement of CH<sub>4</sub> emissions from terrestrial ecosystems in China is not only very important for exploring the impact of climate change on the ecological environment, but also of great significance for the in-depth study of ecosystem carbon cycling. In this study, we used the Emission-Factor Approach to estimate CH<sub>4</sub> emissions from terrestrial ecosystems in China from 2010–2020 and explored the spatial distribution characteristics of CH<sub>4</sub> emissions. The estimated CH<sub>4</sub> emission inventory of terrestrial ecosystems with 0.05 spatial resolution on monthly time scale is in good agreement with the results of the latest emission inventory. It is estimated that CH<sub>4</sub> emissions from terrestrial ecosystems in China are 19.955 Tg yr<sup>-1</sup>, including 18.61% (3.713 Tg yr<sup>-1</sup>) from vegetation, 21.47% (4.285 Tg yr<sup>-1</sup>) from wetlands and 59.92% (11.957 Tg yr<sup>-1</sup>) from paddy fields, with the largest contribution from paddy fields. The regions with high CH<sub>4</sub> emissions from terrestrial ecosystems in China are mainly located in the central, eastern and southeastern regions of China, and show a decreasing trend from southeast to northwest. The CH<sub>4</sub> emission from terrestrial ecosystems in China has obvious seasonal variation characteristics, with the lowest emission in January (0.248 Tg month<sup>-1</sup>) and the highest emission in August (3.602 Tg month<sup>-1</sup>). The emissions are high in summer and autumn and low in spring and winter. CH<sub>4</sub> emissions from terrestrial ecosystems in China showed an overall upward trend from 2010–2020.

**Keywords:** China; terrestrial ecosystem; CH<sub>4</sub> emission inventory; spatiotemporal variations



**Citation:** Yang, Y.; Shi, Y. High Spatial and Temporal Resolution Methane Emissions Inventory from Terrestrial Ecosystems in China, 2010–2020. *Atmosphere* **2022**, *13*, 1966. <https://doi.org/10.3390/atmos13121966>

Academic Editor: James Lee

Received: 29 October 2022

Accepted: 22 November 2022

Published: 25 November 2022

**Publisher's Note:** MDPI stays neutral with regard to jurisdictional claims in published maps and institutional affiliations.



**Copyright:** © 2022 by the authors. Licensee MDPI, Basel, Switzerland. This article is an open access article distributed under the terms and conditions of the Creative Commons Attribution (CC BY) license (<https://creativecommons.org/licenses/by/4.0/>).

## 1. Introduction

Methane (CH<sub>4</sub>) is the second most important greenhouse gas (GHG) in the atmosphere after carbon dioxide (CO<sub>2</sub>), accounting for more than 20% of the total greenhouse gases [1]. According to the Intergovernmental Panel on Climate Change (IPCC) Fifth Assessment Report, the global warming potential of CH<sub>4</sub> is 28 times that of CO<sub>2</sub> over a 100-year period, and its residence time in the atmosphere is about 9.1 years [2]. The latest findings from the World Meteorological Organization's Global Atmosphere Watch Program point out that as of 2019, the average global atmospheric concentration of CH<sub>4</sub> is 1877 ± 2 ppb, reaching 260% of pre-industrial levels, and is still rising at an average rate of 7.3 ppb per year over the last decade. Its radiative forcing contribution to the growth of global radiative forcing of greenhouse gases reaches 16% [3]. Compared with CO<sub>2</sub>, CH<sub>4</sub> has higher global warming potential and shorter retention time in the atmosphere. Compared with controlling CO<sub>2</sub>, quickly and effectively controlling the increase of CH<sub>4</sub> content in the atmosphere can quickly slow down the recent global warming so as to improve the global ecosystem and reduce global economic losses. In addition to climate benefits, reducing CH<sub>4</sub> emissions will also reduce surface ozone generation, which can improve human health and crop production [4,5].

China is located in the high value area of atmospheric CH<sub>4</sub> concentration, so it is of great significance to study and estimate the main sources of atmospheric CH<sub>4</sub> [6,7]. The ecosystem of China is complex and diverse, and it is a key region where Eurasia has a great impact on global climate change. Under the background of climate warming, the measurement of CH<sub>4</sub> emissions from typical terrestrial ecosystems in China is not only very important to explore the impact of climate change on the ecological environment, but also of great significance to the in-depth study of ecosystem carbon cycles. The latest data on the global CH<sub>4</sub> budget from 2000–2017 show that about 40% of global CH<sub>4</sub> emissions to the atmosphere come from natural sources (mainly vegetation and wetlands) and about 60% from anthropogenic sources (mainly paddy fields, livestock, coal mining, municipal solid waste (MSW) treatment and biomass burning) [1]. Among them, vegetation and wetlands in natural sources and paddy fields in anthropogenic sources together constitute terrestrial ecosystems, which are strongly correlated with the environment and have obvious spatial differentiation characteristics and seasonal variation trends. Therefore, a systematic and comprehensive estimation of CH<sub>4</sub> emissions from terrestrial ecosystems in China and the establishment of a CH<sub>4</sub> emission inventory with high spatial and temporal resolution are important for understanding the changes in atmospheric CH<sub>4</sub> concentrations and providing data support for China's emission reduction strategy.

Extensive research has been conducted by domestic and international scholars in estimating emissions from major sources of CH<sub>4</sub> from terrestrial ecosystems in China, such as vegetation [8,9], wetlands [10–12], and paddy fields [13,14]. At the same time, a number of scholars have estimated a comprehensive CH<sub>4</sub> emission inventory in China that includes multiple emission sources [15–19]. Although there have been a large number of studies on the estimation of CH<sub>4</sub> emissions, there are few studies on the estimation of CH<sub>4</sub> emissions from long-term terrestrial ecosystems based on pixel scale and monthly scale in China. Most existing inventories of CH<sub>4</sub> emissions from terrestrial ecosystems in China are estimated based on data from the China Statistical Yearbook, mostly on an annual and provincial basis, which cannot truly reflect the spatially divergent characteristics and seasonal trends of CH<sub>4</sub> emissions [20]. Therefore, based on the published research literature, remote sensing data and existing statistical data, we estimated the monthly CH<sub>4</sub> emissions of China's terrestrial ecosystem from 2010–2020. We also developed a map of CH<sub>4</sub> emissions from terrestrial ecosystems at high spatial resolution (0.05° × 0.05°) monthly time scales in China, which can be used to further explore the spatially divergent characteristics and seasonal trends of CH<sub>4</sub> emissions from terrestrial ecosystems in different regions of China. This high spatiotemporal resolution CH<sub>4</sub> emission inventory can help us to better understand the CH<sub>4</sub> budget of regional terrestrial ecosystems and provide reliable input data for atmospheric transport and chemical models.

## 2. Materials and Methods

The data used in this study are mainly MODIS remote sensing data, meteorological data, and data from others' studies. The data used to estimate CH<sub>4</sub> emissions in this study and their detailed descriptions are shown in Table 1. Since some data have different spatial resolutions, we resampled some data to 0.05° × 0.05° spatial resolution by bilinear interpolation in order to maintain consistency.

**Table 1.** Data used to estimate CH<sub>4</sub> emissions in this study.

Data Set	Required Data	Information
MODIS/Terra Land-Surface Temperature/Emissivity	Surface temperature <sup>1</sup>	0.05° × 0.05°, 2010–2020, monthly
MODIS/Terra + Aqua Land Cover Type L3	Land cover type <sup>2</sup>	0.05° × 0.05°, 2010–2020, yearly
MODIS/Terra Vegetation Indices L3	NDVI <sup>3</sup>	0.05° × 0.05°, 2010–2020, monthly
GPCP (Global Precipitation Climatology Project)	Rainfall <sup>4</sup>	2.5° × 2.5°, 2010–2020, monthly

Table 1. Cont.

Data Set	Required Data	Information
MODIS/Terra Net Primary Production Gap-Filled L4 Spatial distribution map of wetlands in China	Net Primary Production <sup>5</sup> Wetland map <sup>6</sup>	500 m × 500 m, 2010–2020, yearly 1 km × 1 km, 2000
Sunshine hours data in China	Sunshine hours <sup>7</sup>	0.05° × 0.05°, 2010–2020, monthly
Remote sensing monitoring data set of land use status and farmland ripening system in China	Crop type <sup>8</sup>	1 km × 1 km, 2015

<sup>1</sup> From MOD11C3 <https://ladsweb.modaps.eosdis.nasa.gov/> (accessed on 20 December 2021); <sup>2</sup> From MCD12C1 <https://ladsweb.modaps.eosdis.nasa.gov/> (accessed on 21 December 2021); <sup>3</sup> From MOD13C2 <https://ladsweb.modaps.eosdis.nasa.gov/> (accessed on 20 December 2021); <sup>4</sup> From Global Precipitation Climatology Project <https://www.ncei.noaa.gov/data/> (accessed on 21 December 2021); <sup>5</sup> From MOD17A3HGF v061 <https://ladsweb.modaps.eosdis.nasa.gov/> (accessed on 15 March 2022); <sup>6</sup> From [21]; <sup>7</sup> This data is generated by spatial interpolation from the sunshine hours data of surface meteorological stations. Sunshine hours data come from China Meteorological Science data Center <https://data.cma.cn/> (accessed on 22 March 2022); <sup>8</sup> From Resource and Environmental Science and data Center of the Chinese Academy of Sciences <http://www.resdc.cn/Default.aspx> (accessed on 25 March 2022).

The method used to estimate CH<sub>4</sub> emissions from terrestrial ecosystems in China in this study is the emission-factor approach, which is a method proposed by the IPCC to estimate GHG emissions and is widely used today. The basic idea is to construct activity density data and emission factor for each emission source according to the emission inventory list, and use the product of activity density data and emission factor as the emission estimation value of the emission item. The calculation formula is as follows:

$$Emission = \sum (AD_{(i,j)} \times EF_{(i,j)}) \tag{1}$$

where *Emission* is the total CH<sub>4</sub> emission from the current emission source; *i* and *j* are pixel positions; *AD* is activity density data (Specific uses and inputs of individual sources directly related to CH<sub>4</sub> emissions); *EF* is emission factor (the amount of CH<sub>4</sub> gas released per unit of a given emission source, also known as the emission rate). CH<sub>4</sub> emissions from terrestrial ecosystems are the sum of CH<sub>4</sub> emissions from each source. The main sources of CH<sub>4</sub> emissions from terrestrial ecosystems are shown in Figure 1.

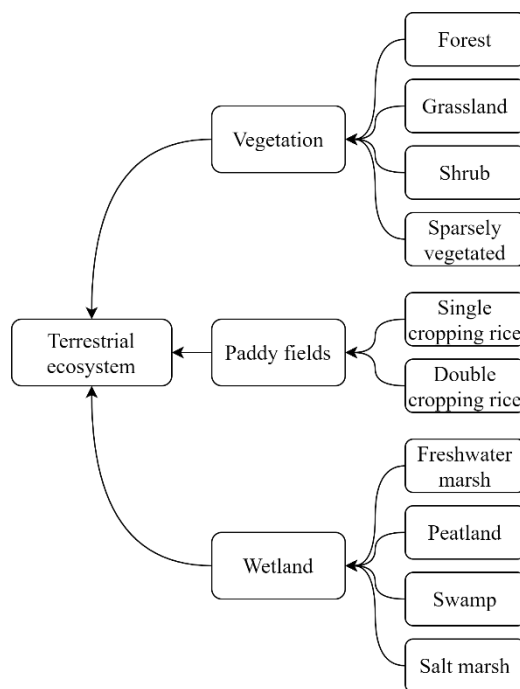


Figure 1. Main sources of CH<sub>4</sub> emission from terrestrial ecosystem in China.

### 2.1. Vegetation

CH<sub>4</sub> has been found to be produced by plants in an aerobic environment, and it is estimated that this contributes 10–30% of the total global emissions [9]. CH<sub>4</sub> is released from normally growing vegetation, as well as from deciduous or dying vegetation, and CH<sub>4</sub> release from vegetation is very sensitive to temperature. Between 30–70 °C, the release of CH<sub>4</sub> approximately doubles for every 10 °C increase in temperature. In addition, the rate of CH<sub>4</sub> emission from both normally growing and decayed phytomasses increased significantly under insolation conditions [22]. The results of the study by Keppler et al. [22] pointed out that the CH<sub>4</sub> emission rates of different plant bodies (normally growing and withered plant bodies) under different light conditions have an exponential relationship with temperature and presented the first equation for estimating vegetation CH<sub>4</sub> emissions. Afterward, Parsons et al. [23] found that replacing net primary productivity (NPP) in Keppler’s model with leaf biomass could improve the estimation accuracy of CH<sub>4</sub> emission from vegetation. In addition, Zhang et al. [8] proposed the conversion relationship between NPP and leaf biomass. Based on the existing research results, Gong et al. [19] integrated the results of Keppler, Parsons and Zhang and improved the estimation method of vegetation CH<sub>4</sub> emissions, which made the estimation results of vegetation CH<sub>4</sub> emissions more accurate. In this study, we use the improved estimation method of Gong et al. The formula is as follows: [19].

$$ER_{mon-liv(i,j,t)} = 198e^{0.023T(i,j,t)} \times h_{sun(i,j,t)} + 30.7e^{0.041T(i,j,t)} \times (24 \times day_t - h_{sun(i,j,t)}), \quad (2)$$

$$ER_{mon-lit(i,j,t)} = 1.6e^{0.05T(i,j,t)} \times h_{sun(i,j,t)} + 0.1e^{0.009T(i,j,t)} \times (24 \times day_t - h_{sun(i,j,t)}), \quad (3)$$

$$biomass_{i,j,t} = 2 \times f_{i,j} \times c_{i,j} \times NPP_{i,j,t} \times 12, \quad (4)$$

$$Emission_{i,j,t} = biomass_{i,j,t} \times (ER_{mon-liv(i,j,t)} + ER_{mon-lit(i,j,t)}) \quad (5)$$

where *i* and *j* represent pixel horizontal and vertical coordinates and *t* represents month; *ER<sub>mon-liv(i,j,t)</sub>* and *ER<sub>mon-lit(i,j,t)</sub>* represent CH<sub>4</sub> emission rates (ng CH<sub>4</sub> g<sup>-1</sup> dry weight month<sup>-1</sup>) of normal growing plants and litter plants, respectively; *T(i, j, t)* stands for surface temperature (°C); *h<sub>sun(i,j,t)</sub>* represents sunshine hours (h month<sup>-1</sup>); *day<sub>t</sub>* denotes the number of days in month *t*; *biomass<sub>i,j,t</sub>* denotes the leaf biomass of vegetation (g m<sup>-2</sup>); *f<sub>i,j</sub>* and *c<sub>i,j</sub>* denote the conversion factors between NPP and biomass and between leaf biomass and biomass, respectively, as shown in Table 2; *Emission<sub>i,j,t</sub>* denotes the CH<sub>4</sub> emission flux from vegetation (mg CH<sub>4</sub> m<sup>-2</sup> month<sup>-1</sup>).

**Table 2.** Conversion factors between leaf biomass and biomass and biomass and NPP for different vegetation types in China.

Vegetation Type	Leaf Biomass/Biomass (c)	Biomass/NPP (f)
Coniferous forest	0.069	9.478
Broadleaf forests	0.055	7.5
Mixed forest	0.063	8.06
Shrubs	0.142	2.633
Grassland	0.341	2.017
Sparse vegetation	0.112	2.0

The data in the table are from the literature [8].

### 2.2. Wetland

CH<sub>4</sub> emission from natural wetlands has obvious seasonal variation, even in places with similar climate, vegetation and topography [24]. Natural wetlands in China can be divided into peatlands, freshwater marshes, swamps and salt marshes, and the CH<sub>4</sub> emission factors vary among different types of wetlands. According to the research results of Ding et al. [10], the relationship between CH<sub>4</sub> emission rate and temperature and

precipitation in different types of natural wetlands is shown in Table 3. Based on the research results of Ding, the equation for CH<sub>4</sub> emissions from wetlands is as follows: [19].

$$Emission_{i,j,t} = type \times day_t \times 24 \times \sum_{k=1}^4 \frac{S_k}{S} \times ER_{k(i,j,t)} \tag{6}$$

where *i* and *j* represent pixel horizontal and vertical coordinates and *t* represents month; *Emission<sub>i,j,t</sub>* indicates wetland CH<sub>4</sub> emission flux; *type* indicates whether the pixel is a wetland (represented by 0 and 1); *day<sub>t</sub>* denotes the number of days in month *t*; *S<sub>k</sub>* is the area of wetland type *k*, and *S* is the total area of all wetland types (obtained by summing the area of four types of wetlands); *ER<sub>k(i,j,t)</sub>* is the CH<sub>4</sub> emission factor of the wetland (Table 3).

**Table 3.** CH<sub>4</sub> Emission factors and area of different types of wetlands in China.

Wetland Type	Area (km <sup>2</sup> )	ER (mg CH <sub>4</sub> m <sup>-2</sup> h <sup>-1</sup> )
Freshwater marsh	24,977	0.663 × <i>T</i> + 2.227 × <i>P</i> − 7.342
Peatland	42,349	2.96
Swamp	2561	0.05
Salt marsh	24,086	0

In the table *T* is the surface temperature and *P* is the rainfall. The data in the table were obtained from the literature [10].

### 2.3. Paddy Fields

The rate of CH<sub>4</sub> emission from paddy fields is related to numerous factors, such as rice irrigation level, soil type, fertilizer application, temperature and tillage practices. Fu et al. [14] estimated rice CH<sub>4</sub> emission factors (Table 4) for each province in China based on rice irrigation level, soil type, fertilizer application and tillage practices. Based on the method provided by IPCC (2006), Gong et al. [19] constructed a model for paddy field CH<sub>4</sub> emissions using vegetation indices to represent rice growth conditions. In this study, we used the model of Gong et al. to estimate CH<sub>4</sub> emissions from paddy fields. We also used the CH<sub>4</sub> emission factors from the paddy fields of Ding et al. The formula is as follows: [19].

$$Emission_{i,j,t} = ER_{k(i,j)} \times \frac{NDVI_{i,j,t}}{mean_k(NDVI_{i,j})} \times day_t \times type_{i,j,k} \tag{7}$$

where *i* and *j* represent pixel horizontal and vertical coordinates and *t* represents month; *k* represents the type of paddy field; *Emission<sub>i,j,t</sub>* is the CH<sub>4</sub> emission flux from paddy field; *ER<sub>k(i,j)</sub>* is the CH<sub>4</sub> emission factor of paddy field; *mean<sub>k</sub>(NDVI<sub>i,j</sub>)* is the mean NDVI value of the current paddy field; *type<sub>i,j,k</sub>* indicates the type of paddy field.

**Table 4.** CH<sub>4</sub> emission factor (ER) of different ripening rice in different provinces of China.

Province	Paddy Field ER (kg CH <sub>4</sub> hm <sup>-2</sup> d <sup>-1</sup> )			Province	Paddy Field ER (kg CH <sub>4</sub> hm <sup>-2</sup> d <sup>-1</sup> )		
	Early Rice	Late Rice	Double Season Rice		Early Rice	Late Rice	Double Season Rice
Beijing	–	–	1.26	Hubei	2.06	3.9	2.06
Tianjin	–	–	1.08	Hunan	1.73	3.41	1.73
Hebei	–	–	1.46	Guangdong	1.77	5.16	1.77
Shanxi	–	–	0.63	Guangxi	1.46	4.91	1.46
Inner Mongolia	–	–	0.85	Hainan	1.58	4.94	1.58
Liaoning	–	–	0.88	Chongqing	0.77	1.85	0.77
Jilin	–	–	0.53	Sichuan	0.77	1.85	0.77
Heilongjiang	–	–	0.79	Guizhou	0.6	2.1	0.6
Shanghai	1.46	2.75	1.46	Yunnan	0.28	0.76	0.28
Jiangsu	1.89	2.76	1.89	Tibet	–	–	0.65
Zhejiang	1.69	3.45	1.69	Shaanxi	–	–	1.19
Anhui	1.97	2.76	1.97	Gansu	–	–	0.65
Fujian	0.91	5.26	0.91	Qinghai	–	–	–
Jiangxi	1.82	4.58	1.82	Ningxia	–	–	0.7
Shandong	–	–	2.0	Xinjiang	–	–	1
Henan	–	–	1.7				

The data in Table 4 come from the literature [19].

### 3. Results

#### 3.1. Spatial Patterns of CH<sub>4</sub> Emissions

The spatial distribution of CH<sub>4</sub> emissions from terrestrial ecosystems in China is shown in Figure 2. The high-value (>18.0 g CH<sub>4</sub> m<sup>-2</sup> yr<sup>-1</sup>) areas of CH<sub>4</sub> emissions from terrestrial ecosystems are mainly located in East and Central China. Combined with Figure 3, it can be seen that the spatial distribution of CH<sub>4</sub> emissions from terrestrial ecosystems in East and Central China are similar to those from paddy fields, indicating that the main source of CH<sub>4</sub> emissions from terrestrial ecosystems in this region is paddy fields. CH<sub>4</sub> emissions from terrestrial ecosystems in Qinghai-Tibet Plateau in China mainly show a point distribution, which is similar to the spatial distribution of CH<sub>4</sub> emissions from wetlands, indicating that wetlands are the main contributors to CH<sub>4</sub> emissions from terrestrial ecosystems in the Qinghai-Tibet Plateau. The regions with low CH<sub>4</sub> emissions (<2.0 g CH<sub>4</sub> m<sup>-2</sup> yr<sup>-1</sup>) in Figure 2 cover almost the whole map, and their spatial distribution is similar to that of vegetation CH<sub>4</sub> emissions in Figure 3, which shows that vegetation CH<sub>4</sub> emissions cover almost the whole region of China, and the CH<sub>4</sub> emissions are high in the southeast region and low in the northwest region. Overall, the regions with high CH<sub>4</sub> emissions (>1.0 g CH<sub>4</sub> m<sup>-2</sup> yr<sup>-1</sup>) from terrestrial ecosystems in China are mainly located in northeastern, central, eastern and southeastern China, with a decreasing trend from southeast to northwest. This trend is similar to that of vegetation coverage, precipitation and temperature from the southeast to the northwest of China.

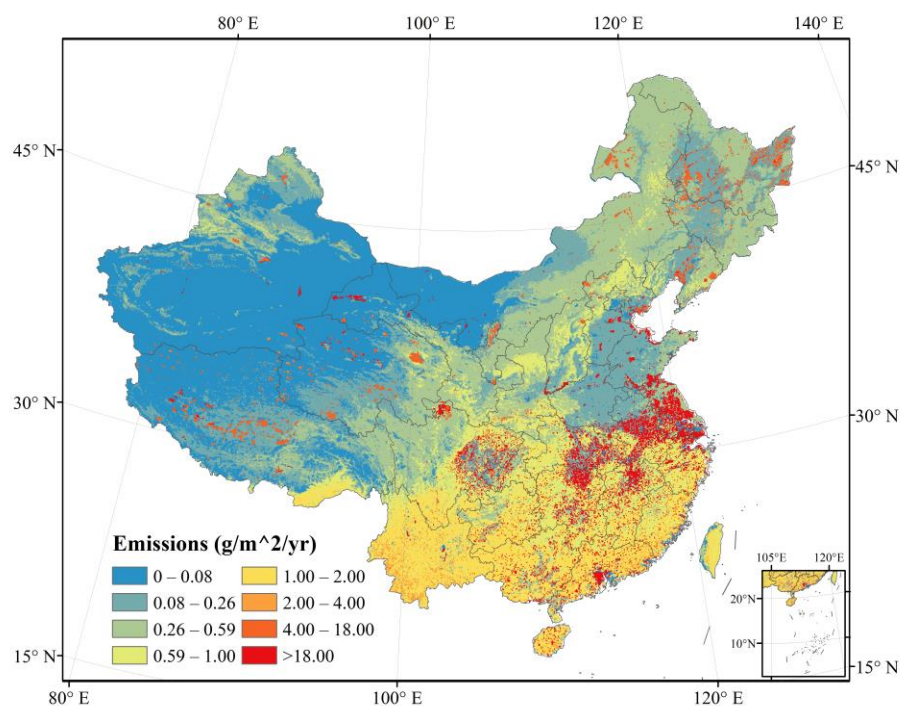


**Figure 2.** Spatial distribution of terrestrial ecosystem CH<sub>4</sub> emission in China.

#### 3.2. Temporal Patterns of CH<sub>4</sub> Emissions

The estimated results show that the average annual CH<sub>4</sub> emission of terrestrial ecosystem in China is 19.955 Tg, in which vegetation, wetland and paddy fields are 3.713 Tg, 4.285 Tg and 11.957 Tg, respectively. The CH<sub>4</sub> contribution of the three major emission sources is 18.61% (vegetation), 21.47% (wetland) and 59.92% (paddy field), respectively. Monthly CH<sub>4</sub> emissions from China's terrestrial ecosystem from 2010–2020 are shown in Table 5.

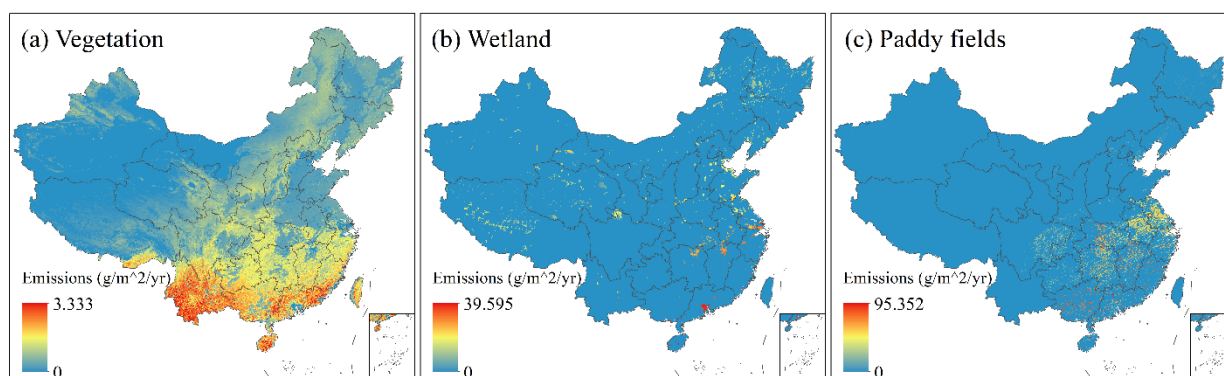


**Figure 3.** (a) Map of CH<sub>4</sub> emissions from vegetation; (b) Map of CH<sub>4</sub> emissions from wetland; (c) Map of CH<sub>4</sub> emissions from paddy fields.

**Table 5.** Monthly and total CH<sub>4</sub> emissions from terrestrial ecosystems in China, 2010–2020.

	Jan.	Feb.	Mar.	Apr.	May.	Jun.	Jul.	Aug.	Sep.	Oct.	Nov.	Dec.	Total
2010	0.262	0.320	0.760	0.968	1.367	2.293	3.535	3.585	3.182	2.575	0.381	0.300	19.530
2011	0.177	0.293	0.675	1.013	1.334	2.375	3.527	3.599	3.125	2.559	0.409	0.249	19.335
2012	0.197	0.252	0.774	1.105	1.415	2.397	3.562	3.599	3.118	2.597	0.375	0.262	19.653
2013	0.242	0.301	0.872	1.070	1.450	2.509	3.612	3.556	3.091	2.573	0.409	0.290	19.977
2014	0.310	0.304	0.911	1.202	1.452	2.468	3.662	3.640	3.229	2.632	0.426	0.273	20.510
2015	0.259	0.302	0.838	1.140	1.418	2.442	3.527	3.603	3.144	2.681	0.387	0.255	19.996
2016	0.255	0.302	0.845	1.166	1.443	2.507	3.595	3.558	3.117	2.700	0.393	0.314	20.194
2017	0.271	0.314	0.768	1.027	1.356	2.245	3.388	3.571	3.303	3.037	0.387	0.286	19.955
2018	0.252	0.272	0.872	1.154	1.463	2.464	3.585	3.628	3.083	2.545	0.403	0.262	19.984
2019	0.236	0.294	0.853	1.156	1.364	2.444	3.565	3.609	3.103	2.534	0.406	0.297	19.861
2020	0.271	0.340	0.919	1.135	1.441	2.566	3.641	3.670	3.207	2.631	0.440	0.245	20.507

The temporal resolution of this study was on a monthly time scale, and the resulting CH<sub>4</sub> emission inventory (Table 5) can be used to explore intra-annual trends in CH<sub>4</sub> emissions from terrestrial ecosystems. CH<sub>4</sub> emissions from terrestrial ecosystems in China have obvious seasonal variation characteristics, with low emissions in spring and winter and high emissions in summer and autumn. As shown in Figure 4, emissions were lowest in January (average 0.248 Tg month<sup>-1</sup>), then gradually increased to a maximum in August (average 3.602 Tg month<sup>-1</sup>) and then gradually decreased to December (average 0.276 Tg month<sup>-1</sup>). The main reason is that CH<sub>4</sub> emission factors from vegetation, wetland and rice emission sources are related to natural factors with seasonal variations, such as temperature, precipitation, sunshine hours, and NPP.

The intra-annual trends of CH<sub>4</sub> emissions from each emission source in terrestrial ecosystems are shown in Figure 4, with significant seasonal variation in CH<sub>4</sub> emissions from vegetation, wetlands and paddy fields. Vegetation CH<sub>4</sub> emissions are related to temperature, biomass, and sunshine hours. The higher the temperature, the longer the sunshine hours, and the greater the vegetation NPP, the higher the CH<sub>4</sub> emissions from vegetation. Emissions are high in July and August because of lush vegetation growth, high temperatures and long sunshine hours, with average emissions reaching 0.430 Tg month<sup>-1</sup>, about 2.7 times higher than emissions in January (0.159 Tg month<sup>-1</sup>). CH<sub>4</sub> emissions from wetlands are mainly affected by temperature and precipitation. The higher the temperature and precipitation, the higher the CH<sub>4</sub> emissions from wetlands. CH<sub>4</sub> emissions from wetlands peaked in July, at an average of 0.684 Tg month<sup>-1</sup>, which was 7.7 times that of January's (average 0.089 Tg month<sup>-1</sup>) because most parts of China had the highest temperatures and precipitation in June, July and August. The paddy field mainly emits CH<sub>4</sub> in the rice growing season, and the CH<sub>4</sub> emission factors of different types of rice are different. The better the rice growth condition, the higher the CH<sub>4</sub> emission. The CH<sub>4</sub> emission factor of late rice (growing mainly from July to October) was higher than that of

early rice (growing mainly from March to June) and double cropping rice mainly emits  $\text{CH}_4$  from June to October, so July to October is the peak of  $\text{CH}_4$  emission from paddy fields. There is no rice cultivation from November to February, so there is no  $\text{CH}_4$  emission from paddy fields during these months.

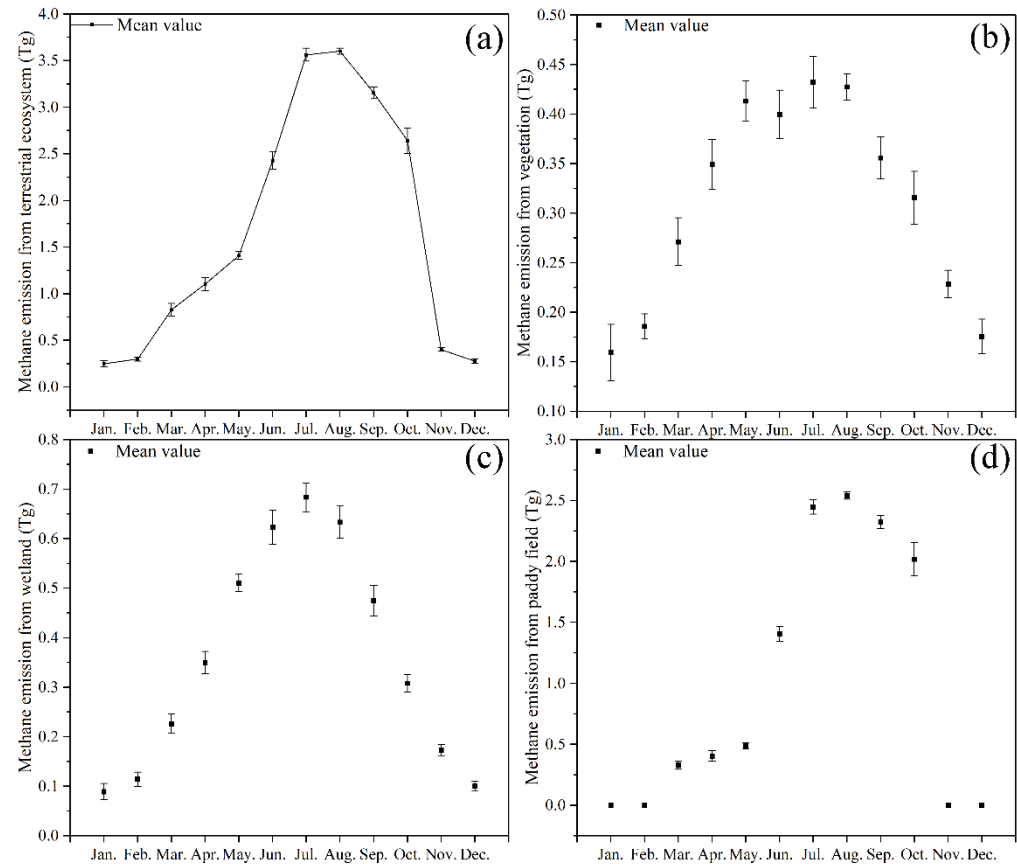


**Figure 4.** (a) Monthly  $\text{CH}_4$  emissions from terrestrial ecosystems; (b) Monthly  $\text{CH}_4$  emissions from vegetation; (c) Monthly  $\text{CH}_4$  emissions from wetland; (d) Monthly  $\text{CH}_4$  emissions from paddy fields.

### 3.3. Intra-Annual Spatial and Temporal Distribution of $\text{CH}_4$ Emissions

The  $\text{CH}_4$  emissions of terrestrial ecosystems not only have obvious seasonal variation characteristics in time, but also have different spatial distribution in different seasons. Figure 5 shows the spatial distribution characteristics of monthly  $\text{CH}_4$  emissions from China's terrestrial ecosystem. It can be seen that in January,  $\text{CH}_4$  emissions were only slightly distributed in China's southern border provinces, and from January to July,  $\text{CH}_4$  emissions gradually extended from south to north, covering most areas of the country in July, and  $\text{CH}_4$  emissions per unit area reached the highest. Since then, it began to fade from north to south from July and August to December, and only a small amount was distributed in the southern border areas, such as the Yunnan and Hainan provinces in December. The main reason for this spatial distribution change is that the temperature, precipitation and vegetation growth in China have similar spatial distribution characteristics in different seasons.  $\text{CH}_4$  emissions from terrestrial ecosystems in China have seasonal spatial distribution characteristics during the year. From spring to winter,  $\text{CH}_4$  emissions show periodic spatial variation characteristics of "from south to north, from north to south".

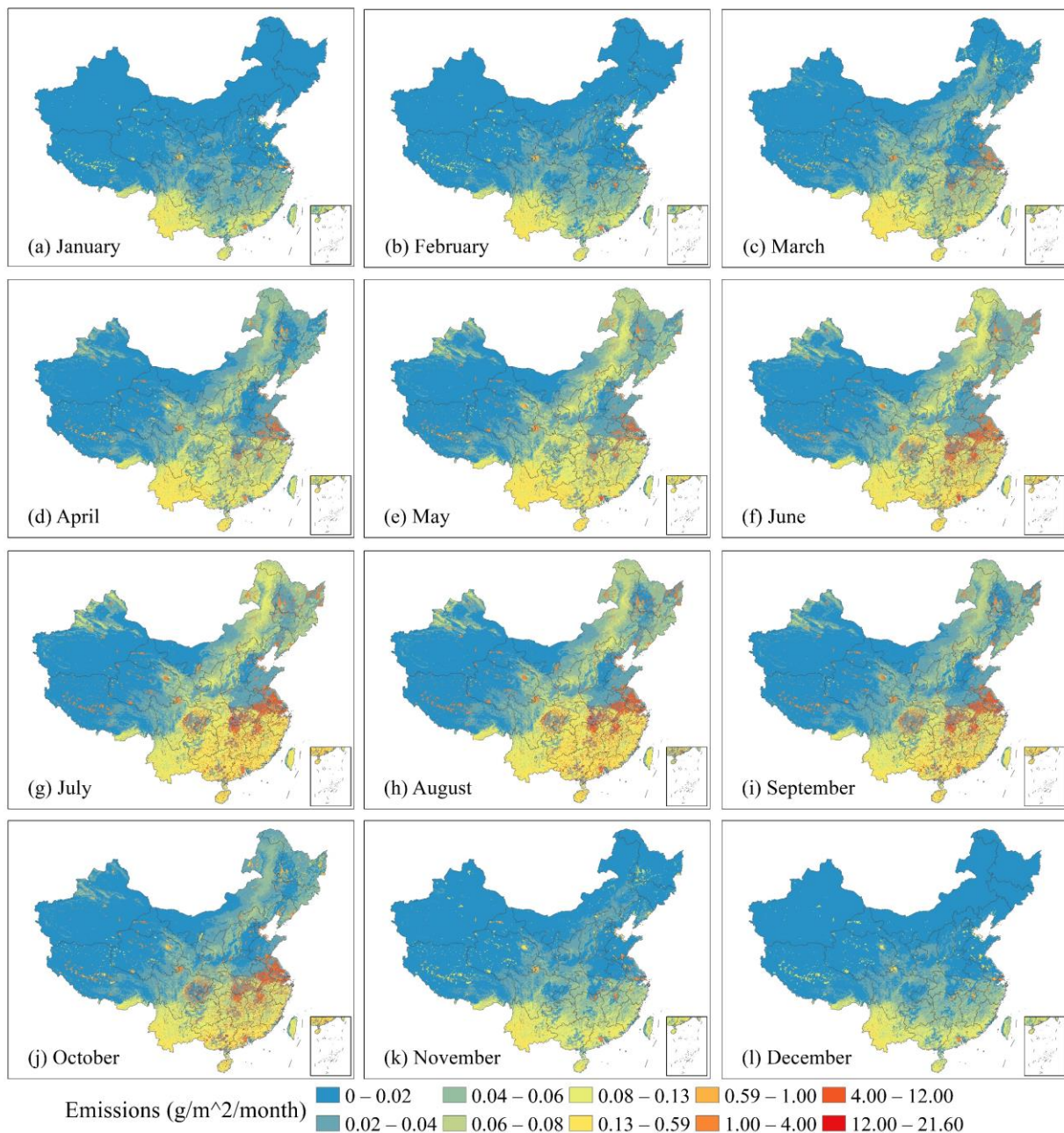


**Figure 5.** (a–l) Monthly  $\text{CH}_4$  emission distribution map of terrestrial ecosystem in China.

We plotted standard deviational ellipses of  $\text{CH}_4$  emissions from terrestrial ecosystems in China for each season as shown in Figure 6. From spring to summer, the center of the ellipse moves to the northeast, and the azimuth of the long axis of the ellipse decreases from  $84.8\text{--}71.4^\circ$ . This indicates that  $\text{CH}_4$  emissions from northern terrestrial ecosystems are increasing in summer and lead to a spatial distribution of  $\text{CH}_4$  emissions close to the “southwest-northeast” direction. At the same time, both the long and short axes of the ellipse are increasing, indicating that the distribution range of  $\text{CH}_4$  emissions is gradually becoming larger from spring to summer. From summer to autumn, the center of the ellipse began to move southward, and both the major axis and the minor axis of the ellipse began to decrease, indicating that the center of gravity of  $\text{CH}_4$  emissions from terrestrial ecosystems began to move southward, and the distribution range of  $\text{CH}_4$  emissions began to narrow. From autumn to winter, the center of the ellipse continues to move southward, and the long and short axes of the ellipse continue to decrease. This indicates that the range

of terrestrial ecosystem CH<sub>4</sub> emissions continues to shrink, and the center of gravity of terrestrial ecosystem CH<sub>4</sub> emissions continues to shift southward.

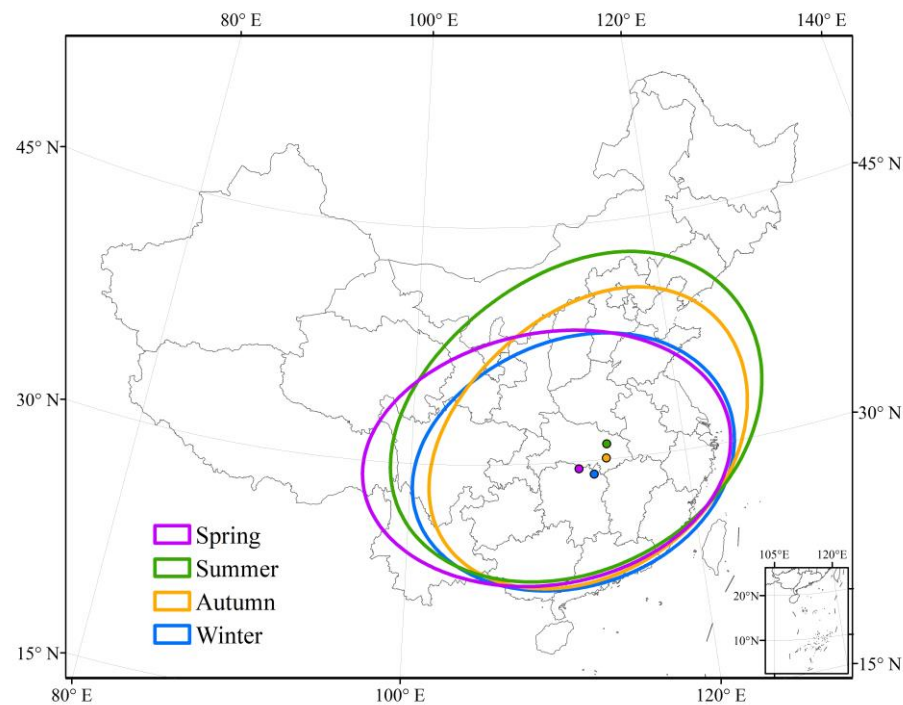


**Figure 6.** Standard deviational ellipse of seasonal variation of CH<sub>4</sub> emission from terrestrial ecosystem in China.

#### 4. Discussion

##### 4.1. Relationship between Interannual Variation Trend of CH<sub>4</sub> Emissions and Air Temperature

In this study, CH<sub>4</sub> emissions from terrestrial ecosystems in China were estimated from 2010–2020, and the interannual trends are shown in Figure 7. It can be seen that the overall CH<sub>4</sub> emissions from terrestrial ecosystems in China are increasing from 2010–2020, with CH<sub>4</sub> emissions peaking in 2014 and 2020. CH<sub>4</sub> emissions grew the fastest between 2011 and 2014, which is consistent with the trend of sustained and rapid increase in average air temperature in China from 2011–2014. The trends in annual mean air temperature in China from 2010–2020 are more consistent with the trends in CH<sub>4</sub> emissions from terrestrial ecosystems in China. Overall, the higher the temperature, the higher the CH<sub>4</sub> emissions from terrestrial ecosystems. The Pearson correlation coefficient  $r$  was calculated for these two sets of data, and an  $r$  of 0.70 was obtained, indicating that the CH<sub>4</sub> emissions from terrestrial ecosystems in China from 2010–2020 were highly linearly correlated with the annual mean air temperature.

##### 4.2. Comparison with the Results of Other Studies

The results of CH<sub>4</sub> emissions from the three major sources of terrestrial ecosystems (vegetation, wetlands and rice) estimated in this study are compared with the results of The People's Republic of China Second Biennial Update Report on Climate Change (CSBUR), Emissions Database for Global Atmospheric Research (EDGAR v5.0, EDGAR v6.0, EDGAR v7.0), The People's Republic of China Third National Communication on Climate Change (CTNC) and other available studies.

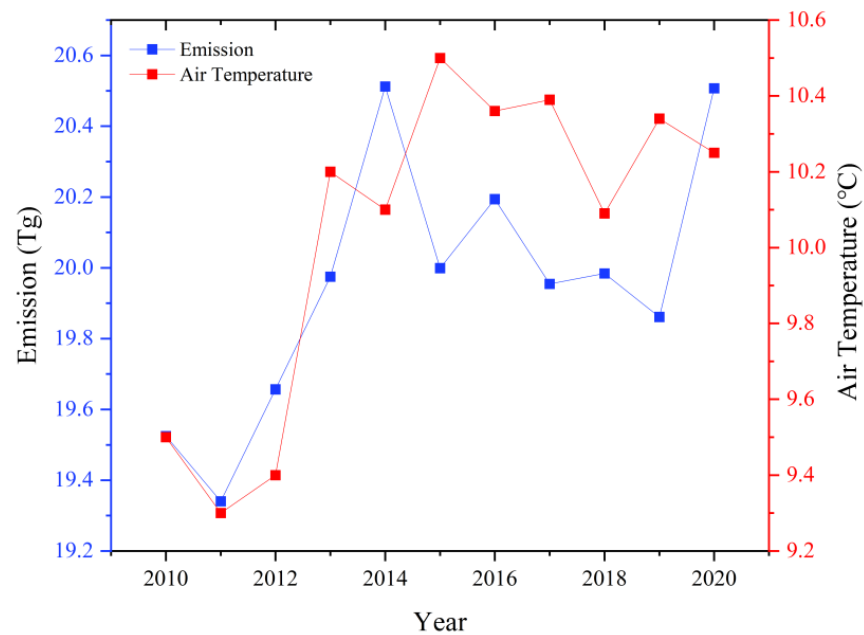


**Figure 7.** Annual methane emission from terrestrial ecosystem and average Air Temperature in China. (China's average Air Temperature data come from China Climate Bulletin from 2010–2020).

On the whole, the estimated results of this study are in good agreement with the research results of the Gong S and Shi Y (2021), EDGARv5.0, EDGARv6.0 and EDGARv7.0 data sets. The vegetation CH<sub>4</sub> emissions in the 2015 results of this study were about 0.82 Tg lower than the vegetation CH<sub>4</sub> emissions in the results of the study by Gong S and Shi Y (2021), and the rice CH<sub>4</sub> emissions were about 0.71 Tg higher than the results of the study by Gong S, Shi Y (2021). The average annual CH<sub>4</sub> emissions from paddy fields in the EDGAR data were about 14 Tg, which was about 2 Tg higher than the results of this study. The estimated CH<sub>4</sub> emissions from wetlands by Huang et al. (2019) and Zhang et al. (2016) were 2.92 Tg (lower than 1.21 Tg in this study) and 4.90 Tg (0.65 Tg higher than in this study). The CH<sub>4</sub> emissions of paddy fields from Huang et al. (2019) and EDGAR dataset were 9.77 Tg (lower than 2.38 Tg in this study) and 14.16 Tg (higher than 2.01 Tg in this study). Gong S and Shi Y (2021) conducted 20,000 Monte Carlo simulations to quantify the uncertainty of CH<sub>4</sub> emission estimates for each emission source with 95% confidence intervals, and calculated emission ranges of 5.67–18.26, 1.98–7.31, and 2.34–6.29 for paddy fields, vegetation, and wetlands [19]. In this study, the method improved by Gong S and Shi Y (2021) is used to estimate CH<sub>4</sub> emissions from vegetation, wetland and paddy fields. The results have higher temporal and spatial resolution, and the estimated results are also within the range of high reliability. As shown in Table 6, this study has comprehensive advantages over other existing studies in terms of spatiotemporal resolution and time series. A total of 40 validation data from other studies had an overall Pearson correlation coefficient of 0.91 with this study (Figure 8). In addition, this study is an emission estimation model based on pixel scale and monthly time scale, and the estimation results of this study are closer to the real situation than the traditional annual emission estimation models.

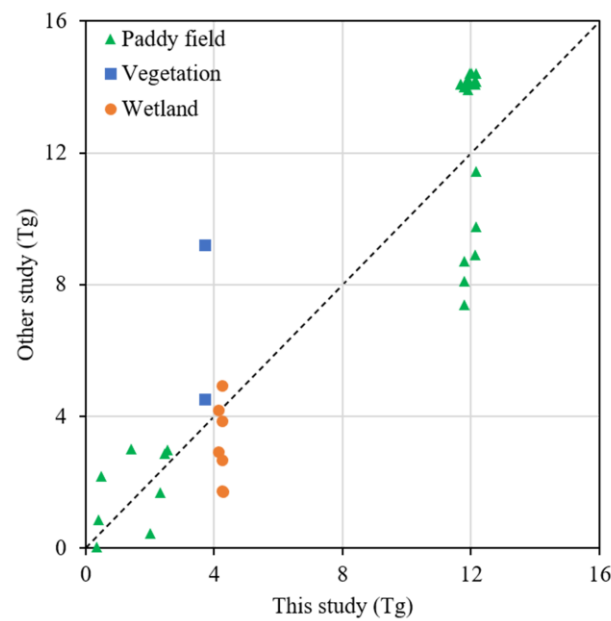


**Figure 8.** The comparison with other studies. Other research data in the figure come from: EDGAR v6.0 [25]; EDGAR v5.0 [26]; Gong et al. (2021) [19]; Huang et al. (2019) [18]; CSBUR [27]; Chen et al. (2013) [28]; Peng et al. (2016) [16]; CTNC [29]; Zhang et al. (2014) [12]; Wei et al. (2016) [30]; EDGAR v7.0 [31].

**Table 6.** Comparison with other research results in spatiotemporal resolution and time series.

	Spatial Resolution	Time Resolution	Time Series
This study	0.05° × 0.05°	Month	2010–2020
EDGAR v7.0 [31]	0.1° × 0.1°	Month	1970–2021
EDGAR v6.0 [25]	0.1° × 0.1°	Month	1970–2018
EDGAR v5.0 [26]	0.1° × 0.1°	Month	1970–2015
Gong et al. (2021) [19]	0.05° × 0.05°	Month	2015
Huang et al. (2019) [18]	Province	Year	2015
Chen et al. (2013) [28]	Province	Year	2008
Peng et al. (2016) [16]	0.1° × 0.1°	Year	1980–2010
Zhang et al. (2014) [12]	Province	Year	2007

In Table 6, Province means that the research results are presented in provincial units.

### 5. Conclusions

In this study, CH<sub>4</sub> emissions from terrestrial ecosystems in China were estimated, and an inventory of CH<sub>4</sub> emissions from gridded 0.05° spatial resolution monthly time scale terrestrial ecosystems was obtained. The inventory is in good agreement with the results of the latest emission inventory, and can be used to partly explain the temporal and spatial variation of atmospheric CH<sub>4</sub> concentration in China. The average annual CH<sub>4</sub> emissions from terrestrial ecosystems in China are estimated to be 19.955 Tg, of which 3.713 Tg, 4.285 Tg and 11.957 Tg are from vegetation, wetlands and paddy fields, respectively. The CH<sub>4</sub> contribution of the three major emission sources is 18.61% (vegetation), 21.47% (wetlands) and 59.92% (paddy fields) respectively, and the paddy fields is the main emission source.

The regions with high CH<sub>4</sub> emissions from terrestrial ecosystems in China are mainly located in the central, eastern and southeastern regions of China and show a decreasing trend from southeast to northwest. CH<sub>4</sub> emission from vegetation is widely distributed, but the emission per unit area is relatively low. High value areas of vegetation CH<sub>4</sub> emissions are mainly located in the southern part of China. The regions with high CH<sub>4</sub> emissions from wetlands are mainly located in the Tibet, Heilongjiang and Qinghai provinces. CH<sub>4</sub> emissions from rice are widely distributed in the south and northeast of China, in which

the middle and lower reaches of the Yangtze River, Pearl River Delta and Chengdu Plain are the main emission areas in the south.

The interannual trends in CH<sub>4</sub> emissions from terrestrial ecosystems in China are very similar to the trends in mean annual air temperature. The correlation coefficient between the two reaches 0.7, and CH<sub>4</sub> emissions are high in years with high average annual temperatures. CH<sub>4</sub> emissions from terrestrial ecosystems in China as a whole continue to increase over the period 2010–2020. CH<sub>4</sub> emissions from terrestrial ecosystems in China have obvious seasonal variation characteristics. Emissions were the lowest in January, with an average of 0.248 Tg, and the highest in August, with an average of 3.602 Tg, about 14.5 times that of January. The overall emissions showed the seasonal characteristics of high in summer and autumn and low in spring and winter. Spatially, CH<sub>4</sub> emissions extend northward from the south, covering almost the entire region of China by July, and then gradually fade from north to south. This is the spatial variation of CH<sub>4</sub> emissions from terrestrial ecosystems in China during the year.

Our estimated CH<sub>4</sub> emission inventory of Chinese terrestrial ecosystem with high temporal and spatial resolution is of great significance to the study of global CH<sub>4</sub> budget, CH<sub>4</sub> traceability, global temperature change, ecosystem carbon cycle in the context of global warming. The inclusion of termite emissions, soil uptake, and permafrost emissions could be considered in subsequent studies to further improve this emission inventory.

**Author Contributions:** Conceptualization, Y.Y. and Y.S.; formal analysis, Y.Y.; methodology, Y.S.; validation, Y.S.; writing—original draft, Y.Y.; writing—review and editing, Y.S. All authors have read and agreed to the published version of the manuscript.

**Funding:** This research was supported by National Key R&D Program of China (2021YFB3901000), the Pioneer Hundred Talents Program of the Chinese Academy of Sciences (Y8YR2200QM), National Natural Science Foundation of China (42071398) and NIES GOSAT-2 Project, Japan.

**Institutional Review Board Statement:** Not applicable.

**Informed Consent Statement:** Not applicable.

**Data Availability Statement:** The sources of data used in this article are detailed in the notes to Table 1. Annual average temperature data for China from China Greenhouse Gas Bulletin <https://www.gov.cn/> (accessed on 25 June 2022).

**Conflicts of Interest:** The authors declare no conflict of interest.

## References

1. Saunois, M.; Stavert, A.R.; Poulter, B.; Bousquet, P.; Canadell, J.G.; Jackson, R.B.; Raymond, P.A.; Dlugokencky, E.J.; Houweling, S.; Patra, P.K.; et al. The Global Methane Budget 2000–2017. *Earth Syst. Sci. Data* **2020**, *12*, 1561–1623. [[CrossRef](#)]
2. IPCC. *IPCC Climate Change 2013: The Physical Science Basis. Contribution of Working Group I to the Fifth Assessment Report of the Intergovernmental Panel on Climate Change*; Cambridge University Press: Cambridge, UK, 2013.
3. WMO Greenhouse Gas Bulletin (GHG Bulletin). No.16: *The State of Greenhouse Gases in the Atmosphere Based on Global Observations through 2019*; World Meteorological Organization: Geneva, Switzerland, 2020; Volume 16, p. 6.
4. Shindell, D.T. Crop Yield Changes Induced by Emissions of Individual Climate-Altering Pollutants. *Earth's Future* **2016**, *4*, 373–380. [[CrossRef](#)]
5. West, J.J.; Smith, S.J.; Silva, R.A.; Naik, V.; Zhang, Y.; Adelman, Z.; Fry, M.M.; Anenberg, S.; Horowitz, L.W.; Lamarque, J.-F. Co-Benefits of Mitigating Global Greenhouse Gas Emissions for Future Air Quality and Human Health. *Nat. Clim. Chang.* **2013**, *3*, 885–889. [[CrossRef](#)]
6. Wu, X.; Zhang, X.; Chuai, X.; Huang, X.; Wang, Z. Long-Term Trends of Atmospheric CH<sub>4</sub> Concentration across China from 2002 to 2016. *Remote Sens.* **2019**, *11*, 538. [[CrossRef](#)]
7. Zhang, G.; Xiao, X.; Dong, J.; Xin, F.; Zhang, Y.; Qin, Y.; Doughty, R.B.; Moore, B. Fingerprint of Rice Paddies in Spatial–Temporal Dynamics of Atmospheric Methane Concentration in Monsoon Asia. *Nat. Commun.* **2020**, *11*, 554. [[CrossRef](#)] [[PubMed](#)]
8. Zhang, X.; Zhang, X.; Zhu, Q.; Jiang, H.; Li, X.; Cheng, M. Spatial distribution simulation and the climate effects of aerobic methane emissions from terrestrial plants in China. *Acta Ecol. Sin.* **2016**, *36*, 580–591.
9. Xie, M.; Li, S.; Jiang, F.; Wang, T. Methane emissions from terrestrial plants over China and their effects on methane concentrations in lower troposphere. *Chin. Sci. Bull.* **2008**, *54*, 2365–2370. [[CrossRef](#)]
10. Ding, W.; Cai, Z.; Wang, D. Preliminary Budget of Methane Emissions from Natural Wetlands in China. *Atmos. Environ.* **2004**, *38*, 751–759. [[CrossRef](#)]

11. Ding, W.-X.; Cai, Z.-C. Methane Emission from Natural Wetlands in China: Summary of Years 1995–2004 Studies. *Pedosphere* **2007**, *17*, 475–486. [[CrossRef](#)]
12. Zhang, X.; Jiang, H. Spatial Variations in Methane Emissions from Natural Wetlands in China. *Int. J. Environ. Sci. Technol.* **2014**, *11*, 77–86. [[CrossRef](#)]
13. Zhang, G.; Xiao, X.; Biradar, C.M.; Dong, J.; Qin, Y.; Menarguez, M.A.; Zhou, Y.; Zhang, Y.; Jin, C.; Wang, J.; et al. Spatiotemporal Patterns of Paddy Rice Croplands in China and India from 2000 to 2015. *Sci. Total Environ.* **2017**, *579*, 82–92. [[CrossRef](#)]
14. Fu, C.; Yu, G. Estimation and Spatiotemporal Analysis of Methane Emissions from Agriculture in China. *Environ. Manag.* **2010**, *46*, 618–632. [[CrossRef](#)] [[PubMed](#)]
15. Zhang, B.; Chen, G.Q. Methane Emissions in China 2007. *Renew. Sustain. Energy Rev.* **2014**, *30*, 886–902. [[CrossRef](#)]
16. Peng, S.; Piao, S.; Bousquet, P.; Ciais, P.; Li, B.; Lin, X.; Tao, S.; Wang, Z.; Zhang, Y.; Zhou, F. Inventory of Anthropogenic Methane Emissions in Mainland China from 1980 to 2010. *Atmos. Chem. Phys.* **2016**, *16*, 14545–14562. [[CrossRef](#)]
17. Ito, A.; Tohjima, Y.; Saito, T.; Umezawa, T.; Hajima, T.; Hirata, R.; Saito, M.; Terao, Y. Methane Budget of East Asia, 1990–2015: A Bottom-up Evaluation. *Sci. Total Environ.* **2019**, *676*, 40–52. [[CrossRef](#)]
18. Huang, M.; Wang, T.; Zhao, X.; Xie, X.; Wang, D. Estimation of atmospheric methane emissions and its spatial distribution in China during 2015. *Acta Sci. Circumst.* **2019**, *39*, 1371–1380.
19. Gong, S.; Shi, Y. Evaluation of Comprehensive Monthly-Gridded Methane Emissions from Natural and Anthropogenic Sources in China. *Sci. Total Environ.* **2021**, *784*, 147116. [[CrossRef](#)]
20. Crippa, M.; Solazzo, E.; Huang, G.; Guizzardi, D.; Koffi, E.; Muntean, M.; Schieberle, C.; Friedrich, R.; Janssens-Maenhout, G. High Resolution Temporal Profiles in the Emissions Database for Global Atmospheric Research. *Sci. Data* **2020**, *7*, 121. [[CrossRef](#)]
21. Ma, K.; You, L.; Liu, J.; Zhang, M. A Hybrid Wetland Map for China: A Synergistic Approach Using Census and Spatially Explicit Datasets. *PLoS ONE* **2012**, *7*, e47814. [[CrossRef](#)]
22. Keppler, F.; Hamilton, J.T.G.; Braß, M.; Röckmann, T. Methane Emissions from Terrestrial Plants under Aerobic Conditions. *Nature* **2006**, *439*, 187–191. [[CrossRef](#)]
23. Parsons, A.J.; Newton, P.C.D.; Clark, H.; Kelliher, F.M. Scaling Methane Emissions from Vegetation. *Trends Ecol. Evol.* **2006**, *21*, 423–424. [[CrossRef](#)]
24. Yan, X.; Ohara, T.; Akimoto, H. Development of Region-Specific Emission Factors and Estimation of Methane Emission from Rice Fields in the East, Southeast and South Asian Countries. *Glob. Chang. Biol.* **2003**, *9*, 237–254. [[CrossRef](#)]
25. European Commission, Joint Research Centre (EC-JRC)/Netherlands Environmental Assessment Agency (PBL). Emissions Database for Global Atmospheric Research (EDGAR), Release EDGAR v6.0\_GHG (1970–2018) of May 2021. Available online: [https://edgar.jrc.ec.europa.eu/dataset\\_ghg60](https://edgar.jrc.ec.europa.eu/dataset_ghg60) (accessed on 25 October 2022).
26. European Commission, Joint Research Centre (EC-JRC)/Netherlands Environmental Assessment Agency (PBL). Emissions Database for Global Atmospheric Research (EDGAR), Release EDGAR v5.0 (1970–2015) of November 2019. Available online: [https://edgar.jrc.ec.europa.eu/overview.php?v=50\\_GHG](https://edgar.jrc.ec.europa.eu/overview.php?v=50_GHG) (accessed on 25 October 2022).
27. The People’s Republic of China Second Biennial Update Report on Climate Change. Available online: [mee.gov.cn](http://mee.gov.cn) (accessed on 25 October 2022).
28. Chen, H.; Zhu, Q.; Peng, C.; Wu, N.; Wang, Y.; Fang, X.; Jiang, H.; Xiang, W.; Chang, J.; Deng, X.; et al. Methane Emissions from Rice Paddies Natural Wetlands, and Lakes in China: Synthesis and New Estimate. *Glob. Chang. Biol.* **2013**, *19*, 19–32. [[CrossRef](#)]
29. The People’s Republic of China Third National Communication on Climate Change. Available online: [mee.gov.cn](http://mee.gov.cn) (accessed on 25 October 2022).
30. Wei, D.; Wang, X. CH<sub>4</sub> Exchanges of the Natural Ecosystems in China during the Past Three Decades: The Role of Wetland Extent and Its Dynamics. *J. Geophys. Res. Biogeosci.* **2016**, *121*, 2445–2463. [[CrossRef](#)]
31. European Commission, Joint Research Centre (EC-JRC)/Netherlands Environmental Assessment Agency (PBL). Emissions Database for Global Atmospheric Research (EDGAR), Release EDGAR v7.0\_FT2021\_GHG (1970–2021) of September 2022. Available online: [https://edgar.jrc.ec.europa.eu/dataset\\_ghg70](https://edgar.jrc.ec.europa.eu/dataset_ghg70) (accessed on 25 October 2022).